

See discussions, stats, and author profiles for this publication at: <https://www.researchgate.net/publication/225559953>

# Dissimilar Joining of Zircaloy-4 to Type 304L Stainless Steel by Friction Welding Process

Article in *Journal of Materials Engineering and Performance* · December 2009

DOI: 10.1007/s11665-009-9376-z

CITATIONS

17

READS

1,576

7 authors, including:



**A. Ravi Shankar**

Indira Gandhi Centre for Atomic Research

63 PUBLICATIONS 835 CITATIONS

[SEE PROFILE](#)



**Sunkavalli Chinna Babu**

Indian Institute of Technology Madras

67 PUBLICATIONS 2,363 CITATIONS

[SEE PROFILE](#)



**Ashfaq Mohammad**

King Saud University

38 PUBLICATIONS 1,129 CITATIONS

[SEE PROFILE](#)



**Kamachi Mudali U.**

VIT Bhopal University

633 PUBLICATIONS 9,284 CITATIONS

[SEE PROFILE](#)

Some of the authors of this publication are also working on these related projects:



metal carbonates:supercapacitor [View project](#)



Thermography [View project](#)

# Dissimilar Joining of Zircaloy-4 to Type 304L Stainless Steel by Friction Welding Process

A. Ravi Shankar, S. Suresh Babu, Mohammed Ashfaq, U. Kamachi Mudali, K. Prasad Rao, N. Saibaba, and Baldev Raj

(Submitted March 5, 2008; in revised form December 16, 2008)

Zirconium- and titanium-based dissolver vessels containing highly radioactive and concentrated corrosive nitric acid solution needs to be joined to the rest of fuel reprocessing plant made of AISI type 304L stainless steel (SS), which demands high integrity and corrosion resistant dissimilar joints. Solid-state joining process of friction welding was proposed in the present work to join zircaloy-4 and type 304L SS since fusion welding processes produce brittle intermetallic precipitates at the interface which reduce the mechanical strength as well as the corrosion resistance of the joint. The present study attempts to optimize joining parameters, without and with thin Ta and Ni interlayers that can prevent brittle intermetallic formation. Tensile test, three-point bend test, and microhardness measurements were performed on the joints. Characterization techniques such as optical microscopy, scanning electron microscopy (SEM), and x-ray diffraction (XRD) were employed. A good friction weld joint of zircaloy-4 to 304L SS was achieved with the joint strength (~540 MPa) greater than that of the base of zircaloy-4, without using any interlayer. A bend ductility of 5° was only obtained without using any interlayer. However, XRD patterns indicated the presence of intermetallics in the friction-welded joints without interlayers. Corrosion test carried out on zircaloy-4 to 304L SS friction joint in boiling 11.5 M nitric acid exhibited corrosion rate of 225 μm/year after 240 h. SEM examination of the corroded joint indicated severe intergranular corrosion attack over stainless steel and preferential dissolution at the interface.

**Keywords** corrosion testing, joining, stainless steels, zircaloy-4

## 1. Introduction

Zircaloy-4 has been proposed as a candidate material for dissolvers and evaporators in a fast reactor fuel reprocessing plant, where highly radioactive and corrosive nitric acid of high concentration and temperatures are used (Ref 1). Zircaloy-4 has been proposed because it has no Ni and has increased Fe content, thus less hydrogen uptake (Ref 2) and also zirconium and its alloys exhibited outstanding corrosion resistance in nitric acid (Ref 1, 3-5). In La Hague reprocessing plant, France, 80 tons of zirconium and 5500 m of piping were employed for the manufacturing of various components like dissolvers, evaporators, heat exchangers, etc. (Ref 5). Therefore, for future fast reactor reprocessing facilities, zircaloy-4 has been proposed as a candidate material for dissolvers and evaporators. The

electrolytic dissolver to be made of zircaloy-4 needs to be connected to the rest of the process vessels and piping made of AISI type 304L austenitic stainless steel, which is extensively used as structural material in reprocessing plants. The fabrication and qualification of this dissimilar metal weld joint are crucial in the reprocessing plant (Ref 6). The design sequence of the dissimilar joining of titanium to 304L SS, which represent welds in dissolver and evaporator in nuclear spent fuel reprocessing plant is discussed elsewhere (Ref 6-8). High integrity dissimilar joints with adequate corrosion resistance, mechanical strength, and bend ductility are essential for uninterrupted operation of reprocessing plants. Dissimilar joints between titanium and stainless steel was achieved by friction welding and explosive welding processes in the earlier work for reprocessing plant applications (Ref 7, 8).

Fusion welding process by electron beam was carried out producing good mechanical properties joints between zircaloy-4 and stainless steel; however, intermetallic and eutectic phases were observed in the molten zone (Ref 9). The secondary phases formed during fusion welding and solidification corrode severely in a corrosive environment and affect the integrity of the joints. Thus dissimilar joints of zircaloy-4 to 304L SS prepared by solid-state joining processes were considered as the best option. Dissimilar joining by solid-state processes was particularly considered for materials with extremely different physical and mechanical properties. Commonly employed dissimilar joining processes are roll bonding, pressure welding, explosive welding, and diffusion bonding. Since no melting occurs at the interface, secondary precipitates are least formed by these processes, and hence the corrosion resistance is not affected significantly during service. Hence, Solid-state joining process such as friction welding was carried out in the present work to join zircaloy-4 to AISI type 304L SS.

A. Ravi Shankar, U. Kamachi Mudali, and Baldev Raj, Corrosion Science and Technology Division, Indira Gandhi Centre for Atomic Research, Kalpakkam 603 102, India; S. Suresh Babu, Department of Metallurgical Engineering, P.S.G. College of Technology, Coimbatore 641 004, India; Mohammed Ashfaq, Department of Metallurgical and Materials Engineering, NIT, Tiruchirappalli 620015, India; K. Prasad Rao, Department of Metallurgical Engineering, IIT Madras, Chennai 600 020, India; and N. Saibaba, Nuclear Fuel Complex, Hyderabad 500 062, India. Contact e-mail: kamachi@igcar.gov.in.

## 2. Experimental Work

### 2.1 Materials

Zircaloy-4 and 304L SS rods of 10 mm diameter and length of 70 mm were used for the experiments. The nominal chemical composition of 304L SS and zircaloy-4 used is given in Table 1.

### 2.2 Friction Welding

The photograph of continuous drive friction-welding machine, shown in Fig. 1, was used in the welding trials which is of 200 KN capacity and can hold workpiece of 6-25.4 mm diameter with variable speed of up to 2400 rpm. The friction pressure, burn off length, and upset time were set to the desired level. The parameters employed for obtaining zircaloy-4 to 304L SS direct joint are tabulated in Table 2. The specimens were polished to obtain fine finish, cleaned with acetone, and pre-etched. During welding, zircaloy-4 was kept in the stationary side and 304L SS in the rotating side. The speed of rotation was kept constant for all the samples at 1500 rpm.

The effect of Ta and Ni as interlayer in improving the joint properties was also attempted. Tantalum foil of thickness 0.15 mm and Ni of 0.75 mm were used in this work because of their metallurgical compatibility with zircaloy-4 and 304L SS. The interlayers were introduced between the rods by making a recess on the zircaloy-4 faying surface and inserting the thin foils. The schematic drawing of sample arrangement depicting the dimensions is shown in Fig. 2. The machined friction-welded rods with good bonding were subjected to liquid penetrant testing, ultrasonic testing, and radiography.

### 2.3 Optical and Scanning Electron Microscopy

Microstructural examinations of the as-received rods and weld interfaces were carried out using a Leica optical microscope and SEM in secondary electron mode. SEM was done on polished and etched surfaces on both the top and transverse section of the welds. SEM examination was also carried out on corroded friction weld joints.

### 2.4 X-Ray Diffraction

X-ray diffraction studies were carried out to confirm the presence of intermetallic formation at the weld interface without interlayer. XRD was carried out with a copper target with a scan range of 20°-80° on the heat affected zone (HAZ) and fractured surface of zircaloy-4.

### 2.5 Microhardness

Matsuzawa Vicker's microhardness machine was used to measure the microhardness across the interface. A load of 150 g was applied for 15 s and the readings were taken from regions on both sides of the 1/4th position and its average values were considered for plotting the graph.

### 2.6 Tensile and Bend Test

Tensile tests for the welded joints were carried out on Universal testing machine. The test specimens were machined and prepared as per ASTM standards for testing (E-8M) with gauge diameter of 7.5 mm and gauge length of 72 mm. A three-point bend test was also carried out on the welded joints with and without interlayer combinations in order to find the bend ductility. The three-point bend test was carried out on

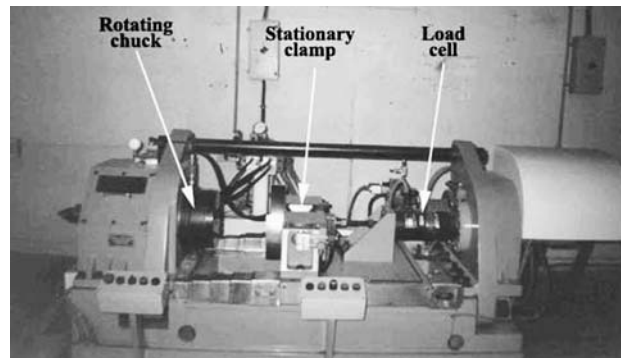


Fig. 1 Photograph of continuous drive friction welding machine

Table 2 Friction weld parameters employed for joining zircaloy-4 to 304L SS

Sample no	Upset force, tone	Friction force, tone	Burn off length, mm	Upset time, s	Total weld time, s	Remarks
<i>Without interlayer</i>						
1	1	0.5	2	3	11.88	Poor joint
2	3	1	2	3	6.89	Poor joint
3	2.5	1	2	3	5.28	Poor joint
4	3	2	1	3	4.56	Better
5	4	2	2	2	4.9	Poor joint
6	4	4	1	3	4.25	Poor joint
7	3	2	1	3	5.6	Better
8	3	3	1	3	4.5	Good
9	3	3	2	3	4.61	Poor joint
10	3	3	1	3	4.34	Good joint
11	3	1	2	3	6.92	Poor joint
<i>With Ni interlayer</i>						
1	2	2	3	3	5.31	Poor joint
2	3	2	3	3	5.34	Poor joint
3	3	3	2	3	4.54	Good joint
<i>With Ta interlayer</i>						
1	3	3	2	3	4.51	Poor joint
2	3	1.5	2	3	4.98	Poor joint
3	2	1.5	2	3	4.72	Poor joint
4	3	3	2	3	4.23	Good joint

Table 1 Nominal Composition of 304L SS and Zircaloy-4 in wt.%

Element	Fe	Cr	Ni	O	N	H	S	P	Sn	C	Si	Mn	Zr
304L SS	Balance	18.33	10.12	...	...	...	0.004	0.030	...	0.03	0.064	1.640	...
Zircaloy-4	0.230	0.114	...	0.113	0.003	0.001	...	...	1.490	0.014	0.008	...	Balance

Universal testing machine having special attachment. The test specimens were machined and prepared as per ASTM standard with 8 mm diameter and 120 mm long. Load was applied exactly at the interface supported at a distance of 60 mm apart from the center.

### 2.7 Corrosion Test

The friction-welded joint sample for corrosion test was polished up to 600 grit emery paper, cleaned with acetone, and weighed before testing. ASTM A262 Practice-C test was carried out on friction-welded joint in 11.5 M nitric acid. The sample was suspended in the boiling 11.5 M nitric acid using Teflon (PTFE) thread for a total period of 240 h. Every 48 h, fresh test solution was used and weight loss measurements were made. The average corrosion rate for five such test periods was calculated in micrometer per year.

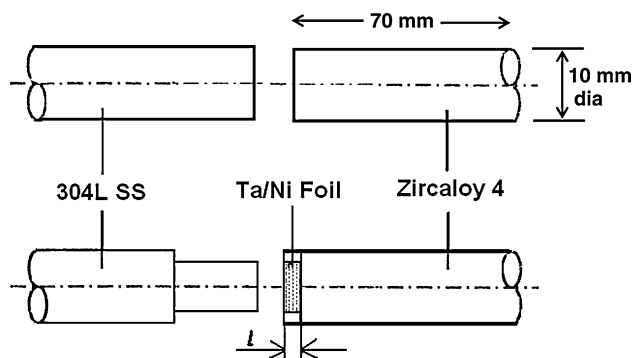


**Fig. 2** Schematic drawing of sample arrangement for friction weld joining

## 3. Results and Discussion

Friction welding involves heat generation through friction and abrasion (by relative motion of two interfaces being joined; rotational speed), heat dissipation (welding/interface temperature), plastic deformation (axial pressure), and chemical diffusion (welding time) (Ref 10). The direct drive friction welding was carried out which consists of a friction phase where heat is generated, a stopping phase where the rotation is terminated, and a forging phase where the pressure is applied to join the pieces (Ref 10). Friction welding carried out with different parameters with and without interlayers for optimizing, resulted in poor joints. However, a friction weld joint with good bonding was obtained between zircaloy-4 and 304L SS at an upset and friction force of 3 tonne and burnoff length of 1 mm without any interlayer. A good friction weld joint was obtained with Ta and Ni interlayer at an upset and friction force of 3 tonne and burnoff length of 2 mm. The results are given in Table 2.

### 3.1 Nondestructive Testing

The machined friction-welded rods were subjected to liquid penetrant testing, ultrasonic testing, and radiography as per ASME section III, and no significant defects were observed.

### 3.2 Optical and SEM Examination

Optical microstructure of the as-received 304L SS, zircaloy-4, and friction weld joint of zircaloy-4 to 304L SS is shown in Fig. 3(a), (b), and (c), respectively. The microstructure in the as-received condition revealed equiaxed grains, while the friction weld joint reveals the thermo-mechanically affected zone (TMAZ). Fine recrystallized grains also known as DRX zone was observed near the interface on zircaloy-4 side due to

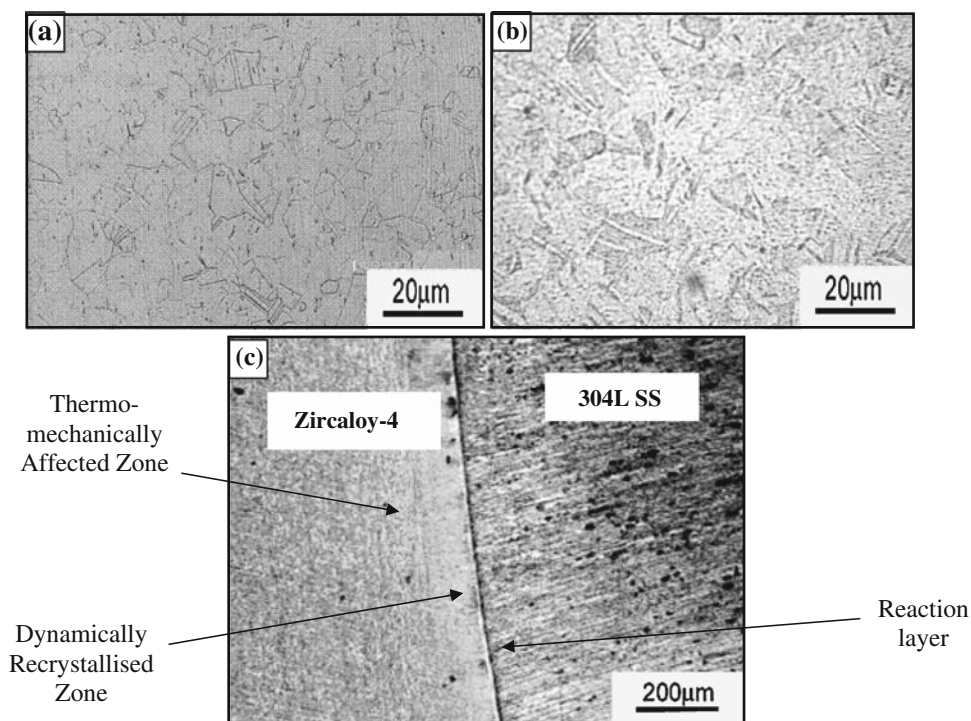


**Fig. 3** Optical micrograph of (a) 304L SS, (b) zircaloy-4 and, (c) friction weld joint of zircaloy-4 to 304L SS

the frictional action, whereas no such region was distinguishable on 304L SS side. This can be explained from the fact that, only zircaloy-4 underwent deformation and participated in flash. Hence, the dynamic recrystallization phenomenon took place in zircaloy-4 side due to the strain involved.

Figure 4(a) and (b) shows SEM micrographs of friction weld interface between zircaloy-4 and 304L SS without interlayer and fractured surface of zircaloy-4, respectively. The interface between zircaloy-4 and 304L SS as shown in Fig. 4(a), is intact without any voids or gaps, and the fractured surface shows brittle fracture (Fig. 4b). Fractograph of zircaloy-4 showing a flat fracture is indicative of fracture along the interface. Small islands of reaction products formed by rubbing of zircaloy-4 against SS 304L also can be seen. Figure 5(a) and (b) shows the SEM micrograph of the friction weld joint with Ni and Ta interlayer at the interface. The micrograph of Tantalum interlayered interface showed a continuous layer of tantalum with varying thickness. The micrograph of the friction weld joint with nickel as interlayer showed more or less continuous layer with microcracks. It was observed that more amount of nickel was pushed toward the steel side through the microcracks. This might have occurred during the upsetting stage. Figure 6(a) and (b) shows SEM micrographs of improper joint with Ni and Ta interlayer of zircaloy-4 to 304L SS friction weld. The fracture mainly occurred at the interface between Ta

interlayer and 304L SS during three-point bend test and is discussed in Section 3.5. Figure 7(a) and (b) shows SEM micrographs of good bonding with Ni and Ta interlayer of zircaloy-4 to 304L SS friction weld.

### 3.3 XRD Results

X-ray diffraction pattern at the HAZ of zircaloy-4 side and fractured surface of zircaloy-4 side are shown in Fig. 8 and 9, respectively. Apart from hexagonal zirconium (05-0665), XRD peaks of brittle intermetallic compounds like  $\text{Ni}_{11}\text{Zr}_9$  (50-0676) and  $\text{Zr}_2\text{Ni}_7$  (71-0543) were found to be matching in the XRD pattern taken from HAZ and from the fractured surface of zircaloy-4. These intermetallics which were formed at the interface were detrimental to the joint properties and facilitated fracture at the interface during three-point bend test. Formation of such intermetallics is also detrimental to the corrosion resistance of the joint at the interface. The formation of such intermetallic compounds at the interface can be minimized by the use of Ta and Ni as interlayer during friction joining of zircaloy-4 and 304L SS.

### 3.4 Microhardness Results

The hardness variation along the interface of zircaloy-4 to 304L SS friction weld joint without interlayer and with Ni and

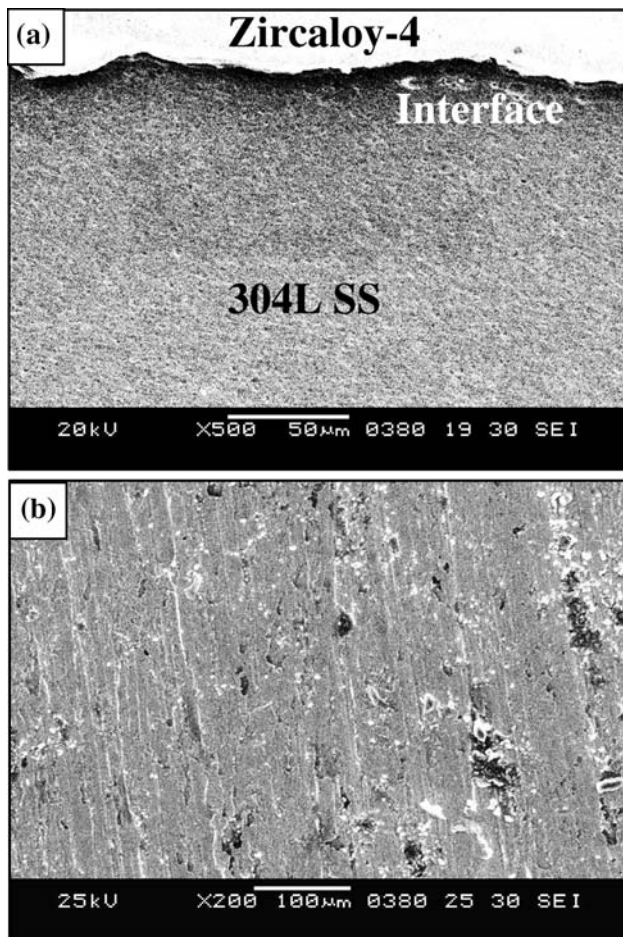


**Fig. 4** SEM micrograph of friction weld joint of zircaloy-4 to 304L SS (a) cross section showing interface and (b) fractured surface of zircaloy-4

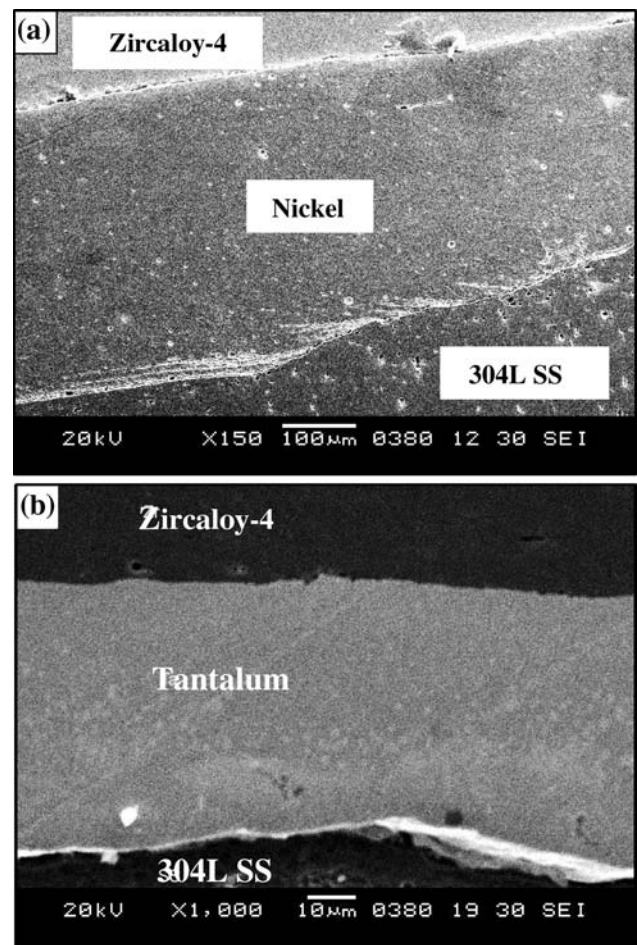


**Fig. 5** SEM micrograph of zircaloy-4 to 304L SS friction weld joint with (a) Ni interlayer and (b) Ta interlayer

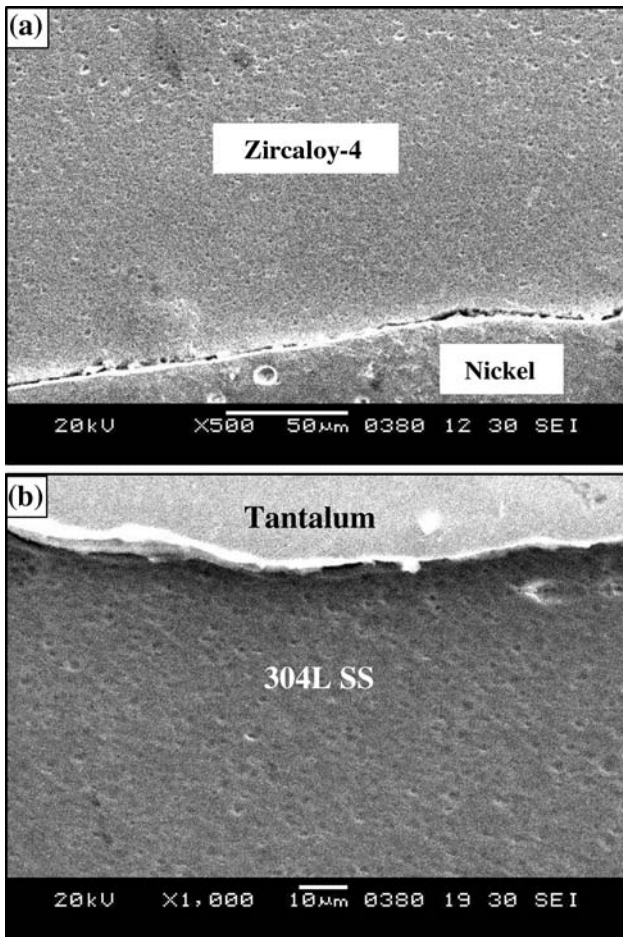


**Fig. 6** SEM micrograph of zircaloy-4 to 304L SS defective friction weld joint with (a) Ni interlayer and (b) Ta interlayer

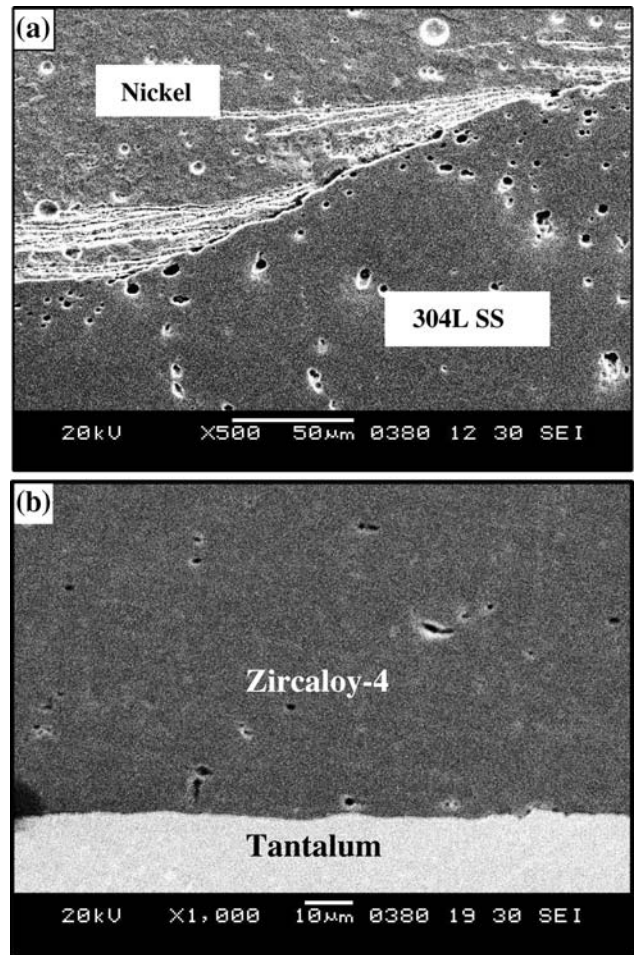


**Fig. 7** SEM micrograph of good zircaloy-4 to 304L SS friction weld joint with (a) Ni interlayer and (b) Ta interlayer

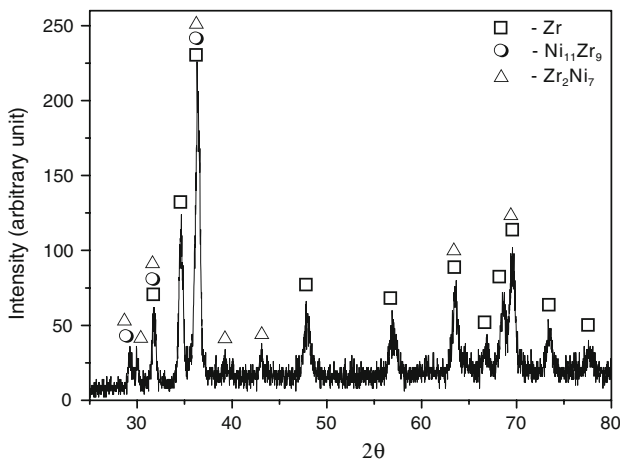


**Fig. 8** XRD pattern of the friction weld joint taken from the HAZ of zircaloy-4

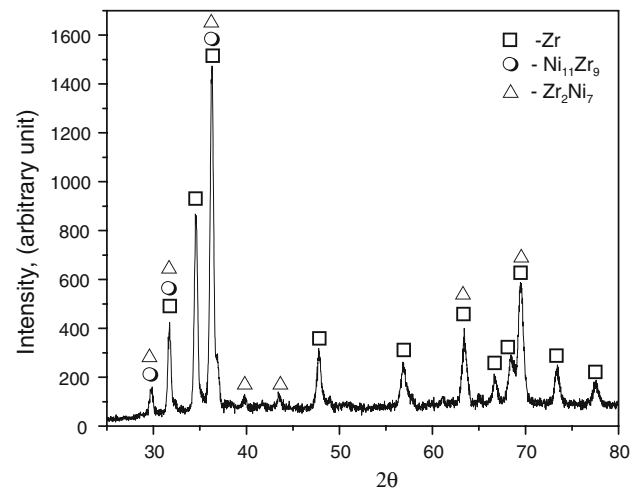


**Fig. 9** XRD pattern of the friction weld joint taken from the fractured surface of zircaloy-4

Ta interlayer is shown in Fig. 10(a), (b), and (c), respectively. On the 304L SS side, there was an increase in hardness from 240 to 290 VHN near the interface with and without interlayer which is due to the strain hardening effect. It was observed that

the hardness of 304L SS to zircaloy-4 near the interface was decreased by 90 VHN from 290 to 180 VHN. There was marginal increase in hardness in the zircaloy-4 side near the interface due to dynamic recrystallization.

### 3.5 Tensile and Bend Test Results

Tensile test of friction weld joints without interlayer exhibited higher tensile strength and ductile fracture in the zircaloy-4 base metal. The average value of fracture load was  $541 \pm 8$  MPa. Based on the tensile test results on friction-welded zircaloy-4 to 304L SS, it was possible to obtain high-strength friction weld joints. From the three-point bend test, the friction-welded zircaloy-4 to 304L SS without interlayer exhibited  $5^\circ$  bend angle at fracture and fracture occurred mainly at the interface. The main cause for the lower bend ductility of zircaloy-4 to 304L SS friction weld joints was due to the formation of intermetallic compounds like  $Zr(Cr,Fe)_2$ ,  $FeZr_4$ , and  $FeZr_2$  as observed from the XRD results. Ahmad et al. (Ref 9) reported the formation of rod shaped  $Zr(Cr,Fe)_2$  intermetallic compound near the HAZ on the stainless steel side of electron beam welded zircaloy-4 to stainless steel joint. Electron beam welding of zircaloy-4 to stainless steel has also produced dendritic structure with  $ZrC_2$ -liquid ( $Zr,Fe$ ) and eutectic phase with  $Zr_2Fe$ - $Zr_2Ni$  (Ref 9). The hardness of  $Zr(Cr,Fe)_2$  phase was found to be three times higher than the average value of the molten zone (Ref 9). The presence of these brittle intermetallic compounds can impair mechanical properties of the joint. Higher bend ductility can be achieved by eliminating the formation of these brittle intermetallic phases or at least by avoiding formation of continuous layers of intermetallic compounds. The three-point bend test on friction weld joints with Ni and Ta interlayers exhibited nil bend angle in the present study. This could be attributed to the higher

thickness of the interlayers used. The mechanical tests on Ti to 304L SS dissimilar joints showed better bend ductility of explosive-welded joint than friction-welded joint although explosive-welded joint showed the bend ductility of only  $106^\circ$  (Ref 6-8). The lower bend ductility was attributed to the combined effect of high hardness of work-hardened Ti in the interface region, and presence of unrelieved residual strain and intermetallics at the interface. The improvement in bend ductility by postweld heat treatment was due to the recovery of cold work at the interface, decrease in hardness of work-hardened Ti in the interface region, and complete bond formation across joint interface (Ref 11). Further improvement in bend ductility of zircaloy-4 to 304L SS friction joint could be achieved by fine tuning of parameters and postweld heat treatment.

### 3.6 Corrosion Test Results

The corrosion test carried out on zircaloy-4 to 304L SS friction joint in 11.5 M nitric acid showed a corrosion rate of  $225 \mu\text{m}/\text{year}$  after 240 h. The corrosion rate was found to increase with time as shown in Fig. 11(a), each data point being the average of three sets. Visual and optical examination of the joint clearly indicated accelerated attack on 304L SS side of the joint. SEM examination also indicated severe intergranular corrosion of the stainless steel (Fig. 11b), which indicates all the corrosion occurred in the 304L SS side only. Dissolution of some intermetallic compounds present at the interface is also shown in Fig. 11(b) which would result in preferential localized

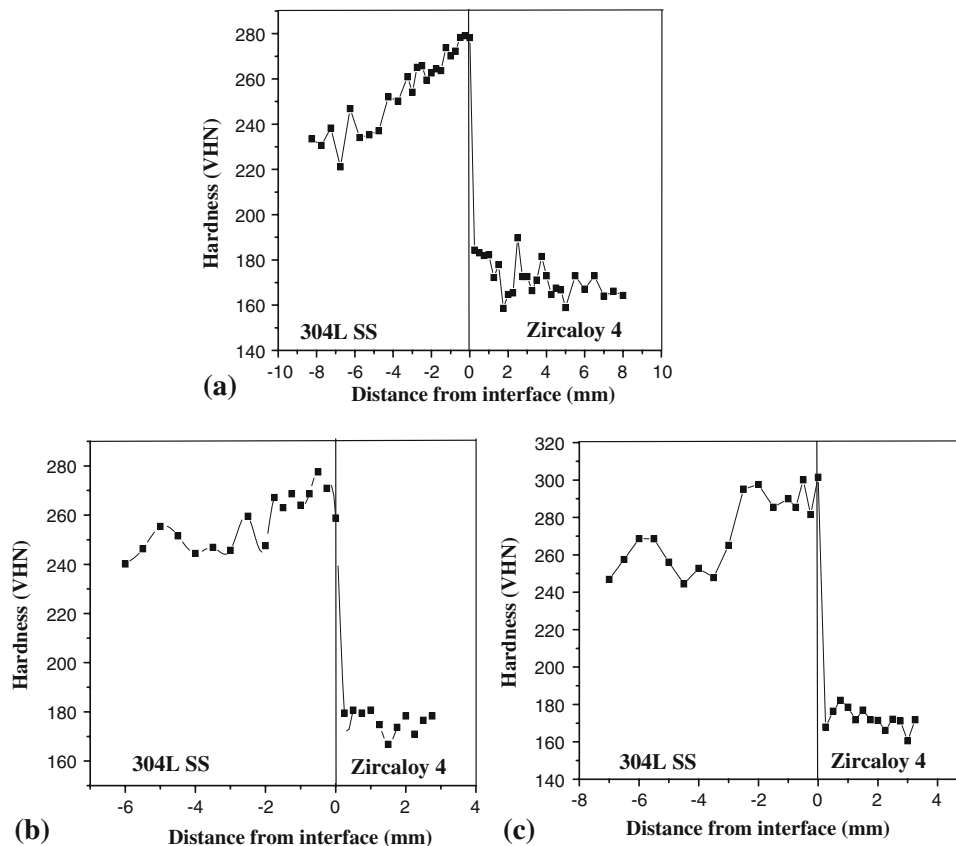


**Fig. 10** Hardness variation along the interface of zircaloy-4 to 304L SS friction weld joint (a) without interlayer, (b) with Ni interlayer, and (c) with Ta interlayer

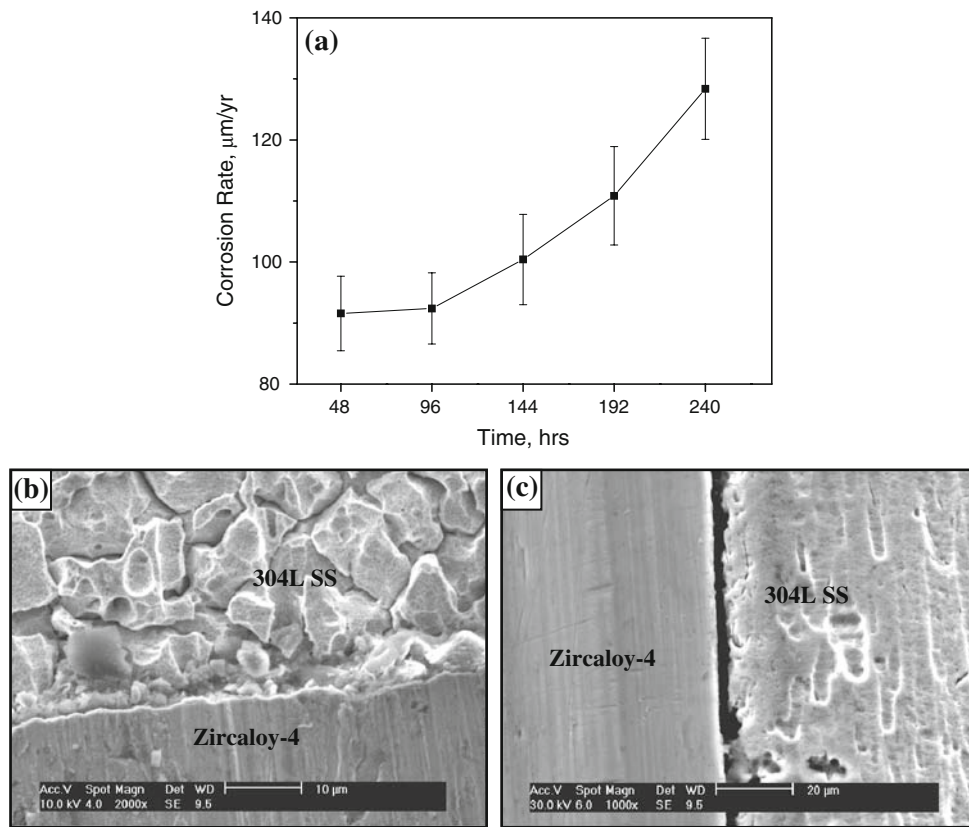


**Fig. 11** (a) Corrosion rate of zircaloy-4 to 304L SS friction weld joint with time (b) and (c) SEM micrograph of friction weld joint exposed to 11.5 M nitric acid for 240 h

corrosion. On the other hand, the corroded surface on zircaloy-4 side showed the presence of smooth and compact film without any attack (Fig. 11b, c). Earlier studies on zircaloy-4 and its welds in 11.5 M nitric acid in liquid, vapor, and condensate phases exhibited superior corrosion resistance as well as the smooth, compact, and adherent,  $\text{ZrO}_2$  surface films on the surface, which protect the alloy from further corrosion (Ref 1). The SEM examination of corroded Ti to 304L SS friction-welded joint indicated severe corrosion attack with wide opening (trench) at the interface (Ref 7) while such trench formation was also observed in zircaloy-4 to 304L SS friction-welded joint in Fig. 11(c). The selective loss of material at the Ti to 304L SS friction weld joint interface was considered unacceptable for structural integrity applications (Ref 7). The localized attack observed at the interface (Fig. 11b, c) may be attributed to the intermetallic dissolution and galvanic corrosion. The desirable microstructure with little or no intermetallic formation, will result in desirable corrosion morphology as shown in Fig. 11(b), while microstructure with a layer of intermetallic formation will result in undesirable trench formation as shown in Fig. 11(c). The friction welding parameters need to be fine tuned in order to avoid the formation of intermetallic compounds at the interface for further improvement of bend ductility and corrosion resistance.

#### 4. Conclusions

The following are the main conclusions drawn on the results of the present investigation:

- (1) A good dissimilar joint between zircaloy-4 and 304L SS was achieved using friction-welding process with higher tensile strength and  $5^\circ$  bend ductility without any interlayer. No improvement in bend ductility was obtained when Ta and Ni were used as interlayers due to higher thickness of Ta and Ni used in the present study.
- (2) Optical and SEM micrograph indicated good joint without any delaminations or voids when joined with and without interlayer.
- (3) XRD patterns indicated the presence of brittle intermetallic compounds like  $\text{Ni}_{11}\text{Zr}_9$  and  $\text{Ni}_7\text{Zr}_2$  in the HAZ and on the fractured surface of friction-welded joint without interlayers.
- (4) Microhardness of the joints with and without interlayers exhibited higher hardness in 304L SS (278 VHN) and lower on zircaloy-4 side (165 VHN).
- (5) Corrosion rate of the friction weld joint as per ASTM A262 Practice-C was found to be around  $225 \mu\text{m/year}$  after 240 h and all the corrosion occurred on the 304L SS side and at the joint interface.

#### References

1. A. Ravi Shankar, V.R. Raju, M. Narayana Rao, U. Kamachi Mudali, H.S. Khatak, and B. Raj, Corrosion of Zircaloy-4 and Its Welds in Nitric Acid Medium, *Corros. Sci.*, 2007, **49**(9), p 3527–3538
2. C.V. Sundaram, Application Related Metallurgy of Zirconium, Niobium and Beryllium, *Trans. Ind. Inst. Metal*, 1986, **39**(1), p 12–27
3. U. Kamachi Mudali, R.K. Dayal, and J.B. Gnanamoorthy, Corrosion Studies on Materials of Construction for Spent Nuclear Fuel Reprocessing Plant Equipment, *J. Nucl. Mater.*, 1993, **203**, p 73–82

4. H. Chauve, J. Decours, R. Demay, M. Pelras, J. Simonnet, and G. Turluer, Zirconium Use for Large Process Components, *IAEA-TECDOC-421*, 1987, p 165–192
5. C. Bernard, J.P. Mouroux, J. Decours, R. Demay, and J. Simonnet, Zirconium Made Equipment for the New La Hague Reprocessing Plants, *Proceedings of the International Conference on Fuel Reprocessing and Waste Management*, Sendai, Japan, RECOD 91, 2, Apr 4–18, 1991, p 570–575
6. B. Raj and U. Kamachi Mudali, Materials Development and Corrosion Problems in Nuclear Fuel Reprocessing Plants, *Progr. Nucl. Energy*, 2006, **48**, p 283–313
7. U. Kamachi Mudali, B.M. Ananda Rao, K. Shanmugam, R. Natarajan, and B. Raj, Corrosion and Microstructural Aspects of Dissimilar Joints of Titanium and Type 304L Stainless Steel, *J. Nucl. Mater.*, 2003, **321**, p 40–48
8. B. Raj, U. Kamachi Mudali, T. Jayakumar, K.V. Kasiviswanathan, and R. Natarajan, Meeting the Challenges Related to Material Issues in Chemical Industries, *Sadhana*, 2000, **25**, p 519–559
9. M. Ahmad, J.I. Akhter, M.A. Shaikh, M. Akhtar, M. Iqbal, and M.A. Chaudhry, Hardness and Microstructural Studies of Electron Beam Welded Joints of Zircaloy-4 and Stainless Steel, *J. Nucl. Mater.*, 2002, **301**, p 118–121
10. J.W. Elmer and D.D. Kautz, Fundamentals of Friction Welding, *ASM Hand Book, Welding, Brazing and Soldering*, Vol. 6, ASM International, Metals Park, OH, USA, 1993, p 150–155, 1993
11. H.C. Dey, V. Shankar, and A.K. Bhaduri, “Titanium/304L Stainless Steel Dissimilar Metal Joint for FRFRP,” IGC Report No. IGC/MTD/MJS/2004/02, May 2004